An unexpected 2-histidine phosphoesterase activity of suppressor of T-cell receptor signaling protein 1 contributes to the suppression of cell signaling

Received for publication, March 18, 2020, and in revised form, April 30, 2020 Published, Papers in Press, May 5, 2020, DOI 10.1074/jbc.RA120.013482

Yue Yin[1], **David Frank**[2], **Weijie Zhou**[1], **Neena Kaur**[2], **Jarrod B. French**[1,3,*], **and Nick Carpino**[2,*]

From the Departments of [1]*Chemistry and* [3]*Biochemistry and Cell Biology, Stony Brook University, Stony Brook, New York, USA, and the* [2]*Department of Microbiology and Immunology, Stony Brook University Medical Center, Stony Brook, New York, USA*

Edited by John M. Denu

The suppressor of T-cell receptor (TCR) signaling (Sts) proteins Sts-1 and Sts-2 suppress receptor-mediated signaling pathways in various immune cells, including the TCR pathway in T cells and the Dectin-1 signaling pathway in phagocytes. As multidomain enzymes, they contain an N-terminal ubiquitin-association domain, a central Src homology 3 domain, and a C-terminal histidine phosphatase domain. Recently, a 2-histidine (2H) phosphoesterase motif was identified within the N-terminal portion of Sts. The 2H phosphoesterase motif defines an evolutionarily ancient protein domain present in several enzymes that hydrolyze cyclic phosphate bonds on different substrates, including cyclic nucleotides. It is characterized by two invariant histidine residues that play a critical role in catalytic activity. Consistent with its assignment as a phosphoesterase, we demonstrate here that the Sts-1 2H phosphoesterase domain displays catalytic, saturable phosphodiesterase activity toward the dinucleotide 2′,3′-cyclic NADP. The enzyme exhibited a high degree of substrate specificity and selectively generated the 3′-nucleotide as the sole product. Sts-1 also had phosphodiesterase catalytic activity toward a 5-mer RNA oligonucleotide containing a 2′,3′-cyclic phosphate group at its 3′ terminus. To investigate the functional significance of Sts-1 2H phosphoesterase activity, we generated His-to-Ala variants and examined their ability to negatively regulate cellular signaling pathways. Substitution of either conserved histidine compromised the ability of Sts-1 to suppress signaling pathways downstream of both the TCR and the Dectin-1 receptor. Our results identify a heretofore unknown cellular enzyme activity associated with Sts-1 and indicate that this catalytic activity is linked to specific cell-signaling outcomes.

A balanced immune response requires the participation of numerous immunoregulatory kinases and phosphatases acting in an oft-opposing manner to provide the optimal level of positive and negative biochemical signals (1–4). Sts-1 and Sts-2 are a pair of homologous phosphatases that share overlapping and redundant functions as negative regulators of immune signaling pathways in a number of different hematopoietic cell types, including T cells (5). The realization that they have a role in regulating T-cell signaling pathways emerged from an analysis of mice lacking Sts expression. In particular, T cells isolated from $Sts^{-/-}$ mice display a pronounced hypersensitivity to T-cell receptor (TCR) stimulation. This is manifested by an increase in TCR-induced proliferation and cytokine production by mutant T cells relative to WT T cells (6). At a biochemical level, the Sts proteins negatively regulate the activation of the TCR-proximal tyrosine kinase Zap-70 (6–8). The Sts proteins also negatively regulate diverse signaling pathways within other cell types, including mast cells, platelets, and bone marrow–derived dendritic cells. For example, Sts-1 has been shown to regulate GPVI–FcRγ signaling in platelets, FcεRI signaling in mast cells, and Dectin-1 signaling in bone marrow–derived dendritic cells by targeting the Zap-70 homologue Syk (9–11). The role of the Sts proteins as critical regulators of immune cell activation pathways is also supported by a large number of genome-wide association studies that link Sts variants within the human population to a number of autoimmune disorders (12–14).

In recent years, it has been shown that the absence of Sts expression can substantially alter the outcome of a pathogen infection. Studies investigating the host immune response to systemic infection by the human fungal pathogen *Candida albicans* demonstrated that, unlike infected WT mice in which extensive fungal proliferation leads to progressive sepsis and rapid lethality, infected $Sts^{-/-}$ mice are substantially resistant (15). $Sts^{-/-}$ mice also display significantly increased survival following infection with Gram-negative *Francisella tularensis* (LVS) (16). Importantly, in response to both pathogens, enhanced microbial clearance within $Sts^{-/-}$ animals was apparent. These results indicate that Sts activity is linked to critical host anti-microbial pathways.

The Sts phosphatases are distinguished from the large number of immunoregulatory protein-tyrosine phosphatases by a unique structure. They have an N-terminal ubiquitin-association (UBA) domain, a central Src-homology 3 (SH3) domain, and a C-terminal histidine-phosphatase (HP) domain, which is named for two conserved catalytic histidines within the active site. The HP domain is structurally and evolutionarily distinct from the phosphatase domain of protein-tyrosine phosphatase enzymes (17) and instead bears a higher degree of homology to a group of structurally related enzymes that hydrolyze phosphate from small molecules such as phosphoglycerate and fructose-2,6-bisphosphate (18). In addition to containing UBA, SH3, and HP domains, the Sts proteins possess a region spanning the UBA and SH3 domains that contains a 2H

This article contains supporting information.

* For correspondence: Nick Carpino, nicholas.carpino@stonybrook.edu; Jarrod B. French, jfrench@umn.edu.

Present address for Jarrod B. French: Hormel Institute, University of Minnesota, Austin, Minnesota, USA.

phosphoesterase motif (19). The 2H phosphoesterase motif contains two conserved histidine residues that are essential for catalytic activity and defines a superfamily of enzymes whose members can be found in all three taxonomic domains. Although the substrates of many 2H phosphoesterases have not been definitely established, many family members exhibit phosphodiesterase activity and have been shown to hydrolyze cyclic phosphodiester bonds present on free nucleotides, oligonucleotides, or at the 3′ termini of RNA. Family members include human myelin 2′,3′-cyclic nucleotide 3′-phosphodiesterase (CNPase) (20), cyclic phosphodiesterase from *Arabidopsis thaliana* (21), *Saccharomyces cerevisiae* tRNA splicing ligase Trl1 (22), and *Escherichia coli* 2′-5′ RNA ligase (23). In spite of considerable differences in primary amino acid sequence, all 2H phosphoesterases have several important features in common. These features include a compact bilobed structure, an active site located within a narrow cleft between the two lobes, and a catalytic core formed in part by two conserved quartets of amino acids (the 2H phosphoesterase motif, H*X*(S/T)*X*, where *X* is any hydrophobic residue) that are arrayed in a 2-fold symmetric conformation with respect to one another (24).

The presence of a putative 2H phosphoesterase motif within Sts prompted us to investigate its functional significance. We determined that each of the two invariant histidines within the Sts-1 2H phosphoesterase motif play an important role in the ability of Sts-1 to function as a negative regulator of cell signaling pathways. We also report the discovery of a novel phosphodiesterase (PDE) catalytic activity associated with Sts-1, derived from the region of Sts-1 located between the UBA and SH3 domains. This catalytic activity is both substrate-specific and stereoselective in nature and depends on the invariant histidines within the 2H phosphoesterase motif. Henceforth, we denote this region the Sts-1 PDE domain. Our results identify a novel enzyme activity associated with Sts-1 and link this novel catalytic activity to specific signaling effects. These findings broaden our understanding of the role that Sts-1 plays in establishing a balanced and productive immune response.

Results

Identification of a functionally relevant 2H-phosphoesterase motif within Sts-1

The 2H phosphoesterase motif is characterized by two identical short amino acid sequences (*HX*(S/T)*X*, where *X* is a hydrophobic residue) that are spaced ~80–85 amino acids apart. Both invariant histidine residues are thought to play an essential role in catalysis (25). The 2H-phosphoesterase domain of human Sts-1 (Sts-1_{PDE}), located between the Sts-1 UBA and SH3 domains, was identified based on two histidine-containing tetrapeptide sequences, HITL and HVTL, that conform to the 2H-phosphoesterase consensus motif (Fig. 1*A*). Sts-2 and Sts evolutionary orthologues also contain an identical domain, with the Sts-2 PDE domain exhibiting 79% homology to hSts-1_{PDE} and the corresponding region of *Drosophila melanogaster* Sts having 73% homology to hSts-1_{PDE} (Fig. 1*A*). However, Sts-1_{PDE} displays very limited homology to other enzymes of the 2H phosphoesterase superfamily, including human CNPase (20), *S. cerevisiae* tRNA ligase (22), *E. coli* 2′-5′ RNA ligase (23), and a putative RNA ligase enzyme from the archeal species *Pyrococcus furiosus* (26) (Fig. 1*A*). This is consistent with previous observations that diverse 2H phosphoesterase enzymes, aside from having the dual histidine–containing tetrapeptide motif in common, display very little overall sequence similarity.

To determine whether Sts-1_{PDE} is critical for Sts-1 intracellular functions, we generated cDNAs encoding two Sts-1 mutants, H126A and H212A, in which the conserved catalytic histidines of the 2H phosphoesterase motif were individually altered to alanine residues. We then examined signaling pathways known to be regulated by Sts-1. Within T cells, the Sts proteins negatively regulate proximal signaling pathways downstream of the TCR (6). NFAT is a transcription factor whose level of activation following TCR engagement depends on the overall strength of activation of signaling pathways downstream of the TCR (27). As previously demonstrated, overexpression of WT Sts-1 in T cells leads to reduced NFAT activation following TCR stimulation, whereas an HP phosphatase-inactive Sts-1 variant (H391N) is ineffective at suppressing TCR signaling (Fig. 1*B*) (28, 29). Similar to Sts-1 H391N, Sts-1 H126A and H212A fail to suppress NFAT activation to the same extent as WT Sts-1 (Fig. 1*B*). This suggests an important role for the Sts-1_{PDE} catalytic histidine residues in negatively regulating TCR signaling in T cells.

Dectin-1 is a C-type lectin receptor involved in the innate immune response to fungal pathogens (30, 31). It is expressed on innate immune cells, engages β-glucan moieties on the surface of different fungal species, and activates downstream innate immune effector pathways, including NFAT, by activating the Zap-70 homologue Syk (32, 33). Signaling pathways downstream of Dectin-1 have been shown to be negatively regulated by the Sts proteins (11). To evaluate a role for Sts-1 PDE domain conserved histidine residues in Sts-1–mediated suppression of C-type lectin receptor signaling, we reconstituted the Dectin-1–Syk signaling axis in 293T cells and compared the ability of WT Sts-1 *versus* PDE domain point mutants H126A or H212A to suppress NFAT activation. Whereas WT Sts-1 negatively regulated zymosan-induced NFAT activation, Sts-1 mutants H126A and H212A each failed to suppress NFAT activation, in spite of equivalent levels of protein expression (Fig. 1*C*). Similar to our observations with the TCR pathway, these results suggest that the conserved histidine residues of Sts-1_{PDE} are necessary for Sts-1–mediated suppression of Dectin-1 signaling.

Enzyme activity of Sts-1_{PDE}

Members of the 2H phosphoesterase family canonically utilize two catalytic histidine residues to cleave a 2′,3′-cyclic phosphodiester linkage of a small molecule substrate. This activity is exemplified by the vertebrate brain 2′,3′-phosphodiesterase (CNPase) (20, 34) that can hydrolyze phosphodiester bonds in cyclic nucleotides, oligonucleotides, and NADcP. In the latter case, the product of the ester hydrolysis reaction is the nucleotide or oligonucleotide with a 2′-phosphate and 3′-hydroxyl group.

To determine whether Sts-1_{PDE} exhibits canonical PDE activity, we first tested whether the protein could hydrolyze the

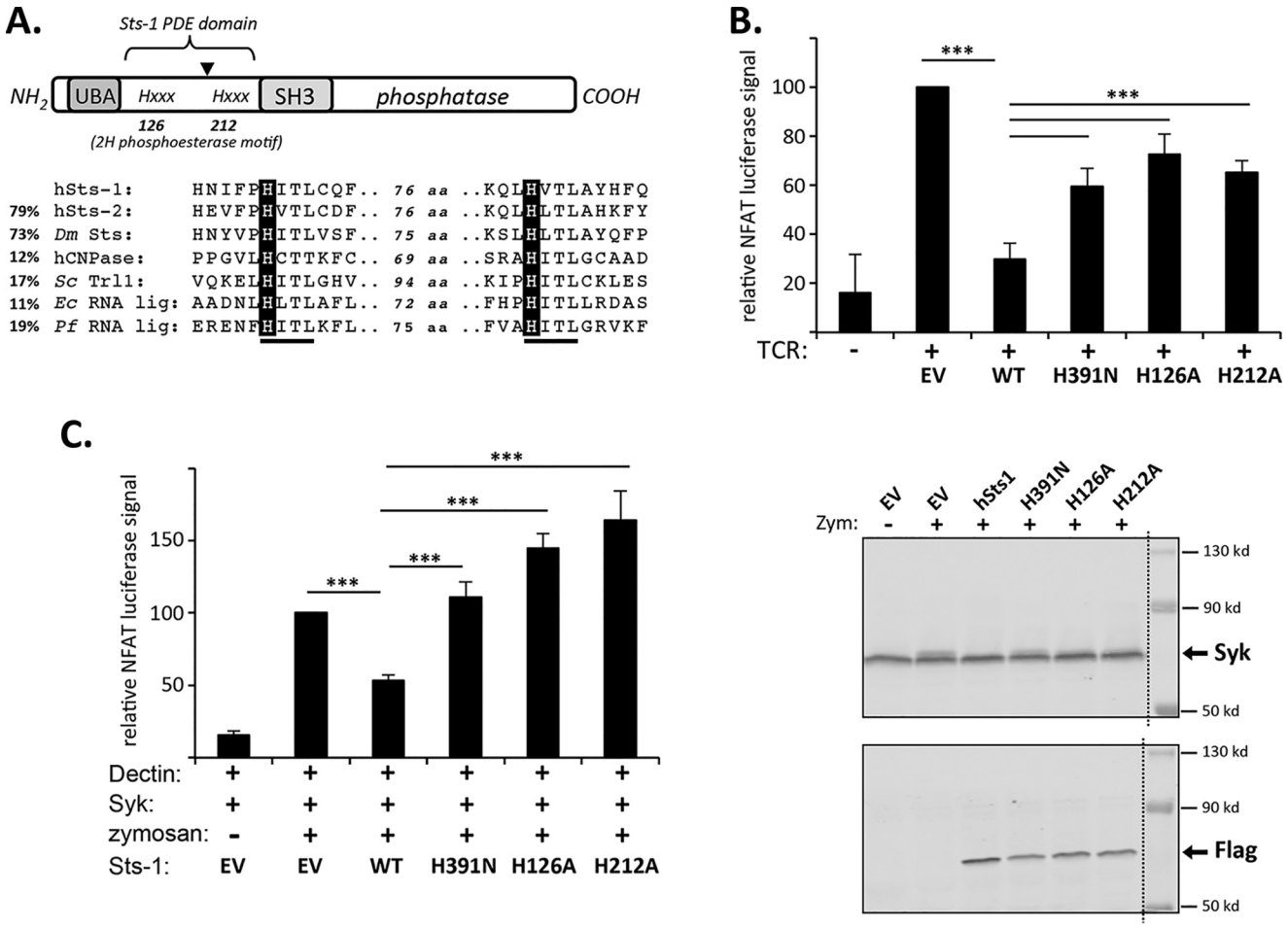

Figure 1. A functional 2H PDE domain within Sts-1. *A*, *top panel*, the Sts-1 PDE domain, located between the UBA and SH3 domains, is defined by the presence of two tetrapeptide sequences His-Xaa-Ser/Thr-Xaa (where Xaa indicates a hydrophobic residue). Within human Sts-1, the catalytic histidine residues are His-126 and His-212. The *triangle* indicates the location of a 39-amino acid insert region present within a splice variant of Sts-2. *Bottom panel*, alignment of the 2H phosphoesterase motif of Sts-1 with the identical region from Sts-2, the *D. melanogaster* Sts orthologue (*Dm Sts*), and four additional 2H phosphoesterase enzymes: human 2′,3′-cyclic-nucleotide 3′-phosphodiesterase (*hCNPase*), *S. cerevisiae* tRNA ligase (*Sc Trl1*), *E. coli* 2′-5′ RNA ligase (*Ec RNA lig*), and *P. furiosus* 2′-5′ RNA ligase (*Pf RNA lig*). % values indicate degrees of homology to hSts-1_{PDE}. *B*, Sts-1 mutants H126A and H212A display impaired regulation of TCR-induced NFAT activation. Jurkat cells transfected to express the indicated Sts-1 proteins and a firefly luciferase reporter construct under the control of NFAT-binding sequences were stimulated for 6 h with anti-TCR antibody and then processed for analysis of luciferase activity. The illustrated results are combined from five separate experiments, each with three replicates. Sts-1 H391A is a phosphatase-inactive mutant of Sts-1. *EV*, empty vector. ***, $p \leq 0.001$ (one-way analysis of variance, Holm–Sidak method). *C*, *left panel*, Sts-1 mutants H126A and H212A display impaired regulation of Dectin-1–induced NFAT activation. 293T cells transfected to express Dectin-1, the indicated Sts-1 proteins, and a luciferase reporter construct under the control of NFAT-binding sequences were stimulated for 4 h with zymosan (*Zym*) and then processed for analysis of luciferase activity. The illustrated results are combined from four separate experiments, each performed in duplicate. ***, $p \leq 0.001$ (one-way analysis of variance, Holm–Sidak method). *Right panel*, representative levels of Syk and FLAG-tagged Sts-1 expression were assessed by Western blotting. Molecular mass marker controls were separated on the *right lane* of the each gel and spliced to the indicated position because of the presence of unnecessary intervening lanes (as indicated by *dotted line*).

phosphodiester linkage in NADcP using a coupled assay that measures the production of 2′-NADP (35). We were unable to observe any enzyme activity for either the full-length Sts-1 protein or the isolated PDE domain, Sts-1_{PDE}. We then developed and utilized an HPLC-based assay to monitor the products of NADcP esterolysis by Sts-1 or Sts-1_{PDE}. Using this assay, we observed enzyme-dependent formation of a product peak over time (Fig. 2*A*). The product that we observed was the 3′-phosphate 3′-NADP, which results from hydrolysis of the 2′-ester linkage (Fig. 2*B*). Analysis of the kinetics of this reaction revealed that this activity saturated with a K_m of 5.4 ± 0.4 mM and a k_{cat} of 0.012 ± 0.003 s^{-1} (Fig. 2*C*). These results stand in contrast to human CNPase, which displays a K_m of 533 ± 56 μM and a k_{cat} of 940 ± 38 s^{-1} for the 3′-phosphodiestease activity that converts 2′,3′-cNADP to 2′-NADP (34). Overall, our results demonstrate that the PDE domain of Sts-1 possesses an enzyme-dependent 2′-phosphodiestease activity for a 2′,3′-cyclic nucleotide substrate.

To confirm the role of the conserved histidines in catalyzing the PDE reaction, we also measured the activity of the H126A and H212A mutants. Both the Sts-1 H126A and Sts-1 H212A had activities barely above the level of noise, turning over at less than 5% the rate of the WT protein (Fig. 2*D*). This is consistent with the proposed essential role in the catalytic mechanism for this pair of conserved histidine residues (25).

Substrate specificity and active site features of Sts-1_{PDE}

Members of the 2′,3′-cyclic phosphodiesterase family of enzymes have been shown to hydrolyze the ester linkage on several types of small molecule, predominantly nucleotides and

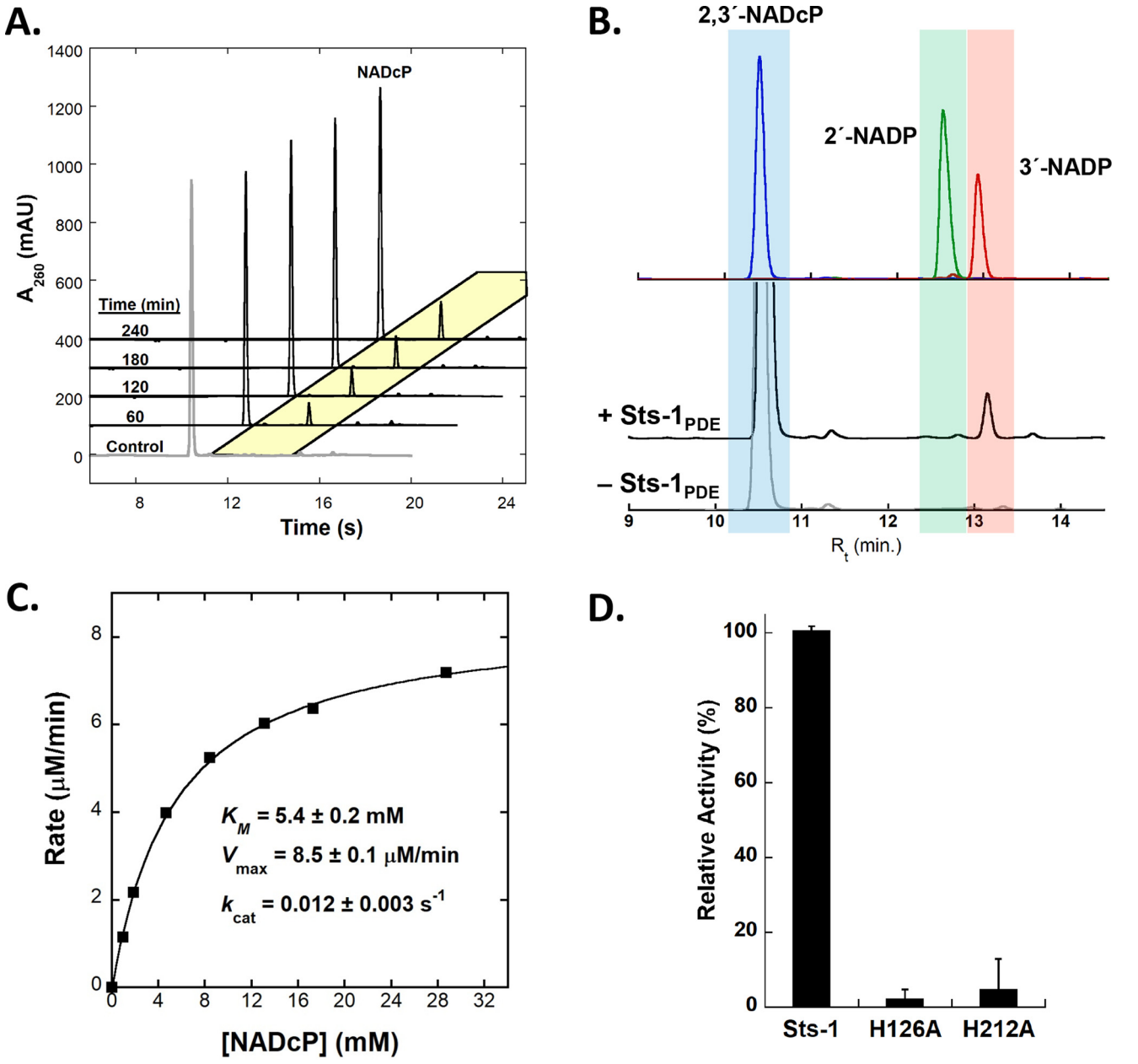

Figure 2. The PDE domain of Sts-1 has 2′,3′-cyclic nucleotide 2′-phospodiesterase activity. *A*, using an HPLC-based assay, the phosphodiesterase activity of Sts-1_{PDE} was tested on the cyclic dinucleotide substrate β-NADH–2′,3′-cyclic monophosphate (NADcP). When compared with the vehicle control, a new peak was observed that increased in size over time when NADcP was treated with Sts-1_{PDE} (shown in the *highlighted region*). *B*, the new peak observed in the choromatograms co-eluted with the 3′-NADP standard (highlighted in *red*; the 2′-NADP standard is highlighted in *green*, and the substrate is highlighted in *blue*). *C*, measurement of the kinetics of the Sts-1_{PDE}–catalyzed esterase activity over a range of substrate concentrations shows that the enzyme saturates and reaches a turnover number of 8.5 μM/min. *D*, the PDE domain of Sts-1 was identified primarily based on the presence of two occurrences of an H*X*(S/T)*X* motif (where *X* is a hydrophobic residue). Mutation of either of these conserved histidine residues to alanine (H126A or H212A) effectively eliminates the esterase activity.

nucleic acids. To determine the breadth and specificity of substrates for Sts-1_{PDE}, we tested over a dozen different nucleotides as possible substrates (Fig. S1). The nucleotides (listed in Table 1) included mononucleotides with 2′,3′- or 3′,5′-cyclic esters and several dinucleotides with varying linkages, including a number of known STING ligands (36, 37). Under the reaction conditions used, only NADcP was a substrate for Sts-1_{PDE} (Table 1). Even 2′,3′-cAMP, which is structurally very similar to NADcP, was not turned over by the enzyme. Ligase activity (formation of any cyclic nucleotides or dinucleotides) was not observed for any of the monophosphates as substrates. Because Sts-1 possesses an HP domain, we also measured phosphatase activity in the context of Sts-1_{PDE} and full-length Sts-1 protein. Although full-length Sts-1 displayed high phosphatase activity, Sts-1_{PDE} exhibited no measureable *p*-nitrophenyl phosphate (pNPP)–hydrolysis activity (Table 1). The PDE activity was not

Table 1
Substrates tested in this work

Substrate tested (concentration)	Sts-1_{PDE}	Sts-1
$NADcP^+$ (1 mM)	0.13 min^{-1}	0.065 min^{-1}
pNPP (phosphatase substrate) (1 mM)	N.D.[a]	98 min^{-1}
2?,3?-cAMP (1 mM)	1.1×10^{-4} min^{-1}	N.D.
2?,3?-cGMP (1 mM)	N.D.	N.T.[b]
2?,3?-cCMP (1 mM)	N.D.	N.T.
3?,5?-cAMP (1 mM)	N.D.	N.T.
3?,5?-cGMP (1 mM)	N.D.	N.T.
pApA (3?,5?) (1 mM)	N.D.	N.T.
c[A(2?,5?)pG(3?,5?)p] (1 mM)	N.D.	N.T.
c[A(3?,5?)pG(2?,5?)p] (1 mM)	N.D.	N.T.
c[A(2?,5?)pA(2?,5?)p] (1 mM)	N.D.	N.T.
c[A(2?,5?)pG(2?,5?)p] (1 mM)	N.D.	N.T.
Cyclic ADP-ribose (1 mM)	N.D.	N.T.
(ligase substrate) (1 mM) 3′ AMP	N.D.	N.T.
(ligase substrate) (1 mM) 3′ GMP	N.D.	N.T.
Substrate (rArArUrArA>P) (20 μM)[c] 2′3′-cRNA	4.4×10^{-3} min^{-1}	5.6×10^{-4} min^{-1}

[a]N.D., no detectable activity at the concentration tested.
[b]N.T., this substrate was not tested with this enzyme.
[c]Note that a lower concentration was used for the cyclic RNA substrate because of poor solubility of the substrate.

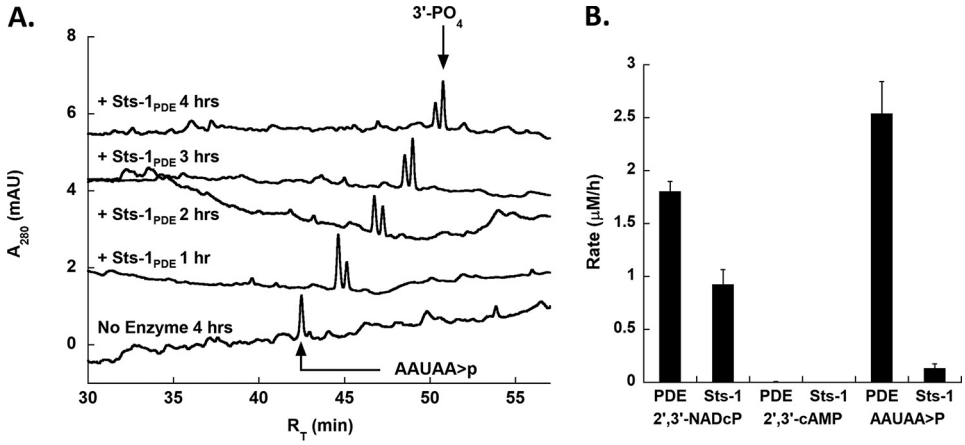

Figure 3. The nucleotide 2′-phosphodiesterase activity of the PDE domain acts upon a cyclic RNA substrate, and the other domains of Sts-1 are implicated in substrate specificity. *A*, when a RNA 5-mer with a 2′,3′-cyclic phosphoester at the terminus (AAUAA>p) was treated with Sts-1_{PDE}, a single new product, the 3′-phosphate (3′-PO_4) product, was generated. The chromatograms show the results of the reaction of the cyclic RNA molecule treated with Sts-1_{PDE} at several time points (+ *Sts-1$_{PDE}$*), and the control reaction shows the cyclic nucleotide treated with vehicle for 4 h (*No Enzyme 4 hrs*). *B*, comparison of the nucleotide phospodiesterase activity of the full-length Sts-1 protein (*Sts-1*) with that of the isolated PDE domain (*PDE*) for several substrates illustrates the selectivity of the active site and the possible role of other Sts-1 protein domains. Although neither form of the enzyme turns over 2′,3′-cAMP at an appreciable rate, the PDE domain has a slightly higher activity for the cyclic RNA substrate (AAUAA>P) than the full-length protein. The full-length Sts-1 catalyzes the esterolysis of NADcP nearly 10-fold faster than with the cyclic RNA substrate.

measurably different over a range of temperatures (20–40 °C), nor was it affected by preincubation of the enzyme with divalent cations. In sum, our results suggest that Sts-1_{PDE} possesses a high degree of substrate selectivity with regard to its ability to target cyclic phosphorylated substrates.

As many of the cyclic PDE enzymes act upon nucleic acid substrates, we next tested the activity of Sts-1_{PDE} on a 2′,3′-cyclic RNA substrate. We treated an RNA 5-mer (rArArUrArA) bearing a 2′,3′-cyclic phosphate terminus with Sts-1_{PDE} and examined the resulting products with our HPLC-based assay. A new peak that co-eluted with the 3′-phosphate standard was observed (Fig. 3*A*). This confirms that the Sts-1_{PDE} has 2′,3′-cyclic PDE activity that selectively cleaves the 2′-phosphoester bond. In addition, this shows that this enzyme can take both a small molecule nucleotide (NADcP) and an RNA oligonucleotide as a substrate. Although solubility limitations of the RNA substrate preclude a complete investigation, the kinetics of this reaction were observed to be relatively slow.

To further analyze substrate selectivity, we compared the PDE activity of full-length Sts-1 protein to the Sts-1_{PDE} isolated domain. Under the same reaction conditions, the full-length protein had a significantly reduced activity for the cyclic RNA substrate, turning over at a 20-fold lower rate than the PDE domain alone (Fig. 3*B*). The rate for NADcP turnover was similar for the two proteins, with less than 2-fold difference.

Sts-1 PDE domain biological activity

In response to TCR stimulation, T cells that lack the Sts proteins hyperproliferate and secrete excessive levels of cytokines, including IFNγ (38). Reconstitution of *Sts*$^{-/-}$ mutant T cells with WT Sts-1 suppresses the hyper-responsive phenotype, whereas reconstitution with Sts-1 variants containing UBA, SH3, or HP domain–inactivating mutations does not suppress the Sts$^{-/-}$ hypersensitivity phenotype (28, 29). To assess a functional role for the PDE domain of Sts-1, we isolated T cells from *Sts*$^{-/-}$ mice and reconstituted them with equivalent levels

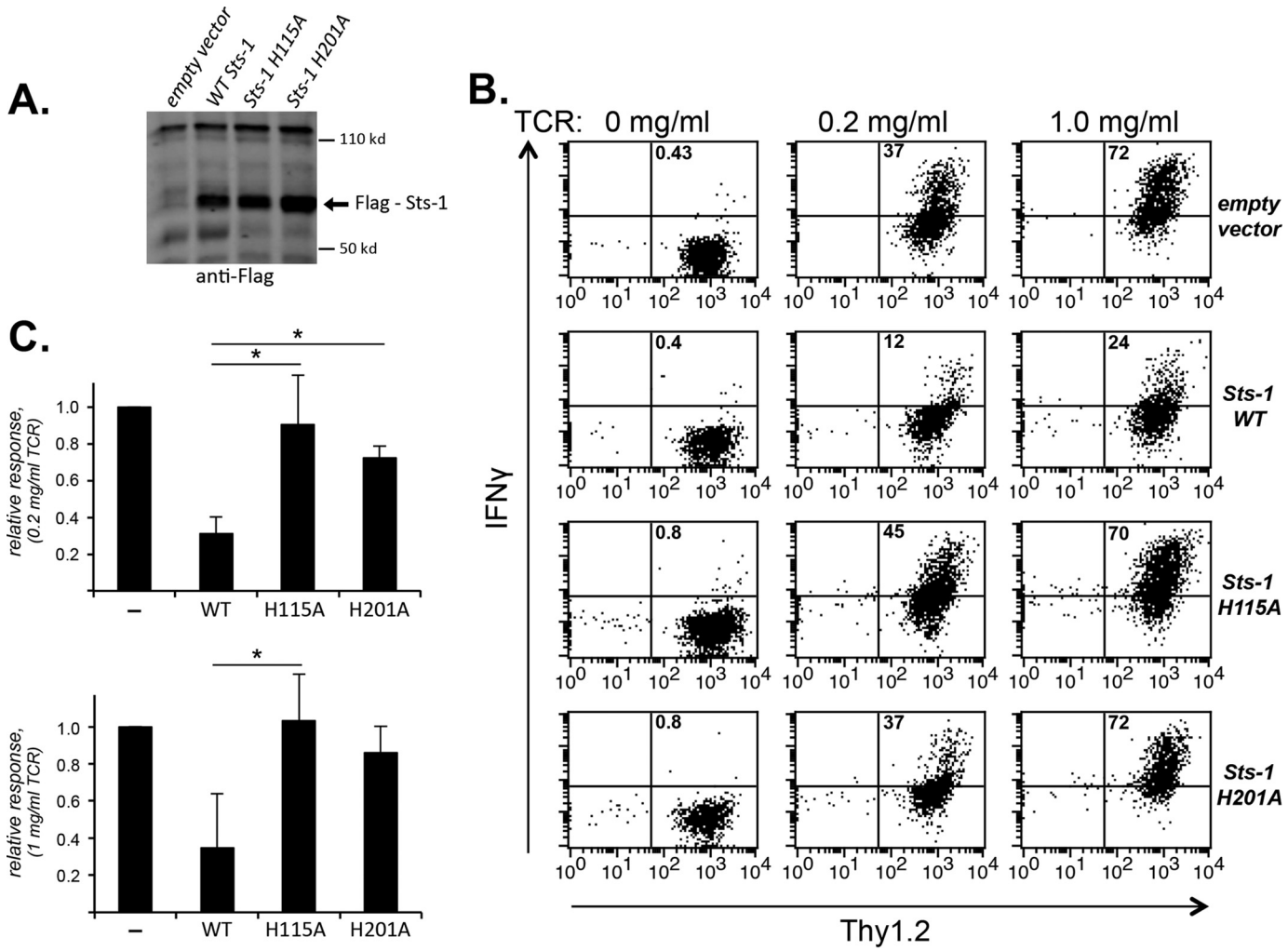

Figure 4. Requirement for Sts-1 2H phosphoesterase catalytic residues in the regulation of IFNγ expression in primary T cells. *A*, levels of expression of murine Sts-1 and PDE mutants H115A and H201A in primary *Sts*$^{-/-}$ T cells, following retroviral-mediated reconstitution. *B* and *C*, primary T cells infected with retrovirus expressing empty vector, WT Sts-1, Sts-1 H115A, or Sts-1 H201A were stimulated for 4 h with the indicated concentrations of anti-TCR stimulatory antibody, and levels of intracellular IFNγ were determined by flow cytometry. Cytokine-expressing T cells are visible in the *upper right quadrant*, with the percentage of cells indicated. Illustrated are representative data (*B*) or the averages of three independent experiments (*C*). *, $p \leq 0.05$.

of WT Sts-1 or PDE mutants H115A and H210A (murine Sts-1 protein numbering) (Fig. 4*A*). Unlike WT Sts-1, Sts-1 H115A and Sts-1 H210A each failed to efficiently suppress IFNγ production (Fig. 4*B*). Their inability to suppress IFNγ production to the same extent as WT Sts-1 was evident over a range of stimulatory antibody concentrations (Fig. 4, *B* and *C*). These results suggest an important role for the critical catalytic residues of the Sts-1 2H phosphoesterase motif in the regulation of IFNγ production by primary T cells and support the hypothesis that Sts-1 PDE activity is important for the function of Sts as a negative regulator of T-cell biological responses.

Discussion

A number of studies have identified the Sts proteins as negative regulators of key signaling pathways, with the unique Sts C-terminal phosphatase domain playing a prominent role in their molecular mechanism of action (29). Importantly, the Sts UBA and SH3 domains have also been shown to play nonredundant functional roles. Indeed, in a current model of Sts intracellular activity, the UBA and SH3 protein-interaction domains are proposed to localize the phosphatase domain to putative intracellular substrates such as activated Syk or Zap-70 (7). This present study identifies a fourth functional domain within Sts-1 that is located between the UBA and SH3 domains, a domain that we refer to as the Sts-1 PDE domain. Preliminary analysis suggests that Sts-1_{PDE} functions to inhibit the activation of signaling pathways downstream of select surface receptors.

Our investigation was prompted by the observation that a region within the N terminus of Sts-1 contains two short sequence motifs that define membership in a superfamily of diverse enzymes known as 2H phosphoesterases. Interestingly, many 2H phosphoesterases have been shown to have an associated cyclic nucleotide PDE activity (19, 24). For example, myelin-associated CNPase produces 2′-AMP from 2′,3′-cAMP (20), cyclic phosphodiesterase from *A. thaliana* cleaves the cyclic phosphate bond of ADP-ribose 1′,2′-cyclic phosphate (21), and yeast Trl1 hydrolyzes the 2′,3′-cyclic nucleotide bond that is formed on the 5′-oligonucleotide half-molecule during

splicing reactions that remove tRNA introns (22). In keeping with the presence of a 2H phosphoesterase catalytic signature within Sts-1, we demonstrated that it possesses an associated cyclic nucleotide PDE enzymatic activity. Our analysis revealed that Sts-1_{PDE} has activity consistent with a 2′,3′-cyclic-nucleotide 2′-phosphodiesterase (EC 3.1.4.16). This specific chemistry has been observed in several prokaryotic species, and the 3′-PDE activity (CNPase; EC 3.1.4.37) is well-known in many organisms, including humans. The observed 2′-PDE activity, however, is relatively unprecedented in humans (39).

Because the Sts proteins have very minimal amino acid sequence similarity to other 2H phosphoesterase family members, there is little in the Sts-1 primary sequence that offers insights into potential substrates. For example, although structural analysis of CNPase has identified amino acids important for its interactions with 2′,3′-AMP, the same substrate specificity determinants are not conserved within the Sts proteins (34). Our data clearly indicate that the Sts-1_{PDE} active site can differentiate between subtle differences in substrate structure. The data showing that NADcP is turned over by the enzyme, whereas the structurally similar 2′,3′-cAMP is not a substrate suggests that a larger, perhaps polynucleotide substrate, is necessary for binding or efficient catalysis. Complicating this is the observation that the larger, 2′,3′-cyclic RNA substrate, although turned over reasonably well by Sts-1_{PDE}, is a much poorer substrate in the context of the intact Sts-1 protein. This could indicate that some other domain of the protein plays a role in defining substrate specificity and perhaps influences catalytic efficiency. It is also possible that the contribution from other domains within the protein is substrate-specific and that selectivity may be more or less pronounced in the context of the native substrate(s).

The Sts-1 PDE reaction mechanism also remains to be elucidated. Although putative reaction mechanisms have been proposed for 2H-phosphoesterase enzymes (21–23, 40), the low sequence similarity to other PDE family proteins, the lack of structural information, and the unusual 2′-PDE activity make the assignment of any particular mechanism to Sts-1_{PDE} nontrivial. One proposed mechanism for 2H-PDE enzymes involves a direct, one-step ligation (or direct hydrolysis) of the 2′,3′-cyclic nucleotide, typically yielding the 3′-product (23, 40). In this case, the active-site histidine residues act predominantly to position the substrate and activate the water molecule for nucleophilic attack. Alternatively, in the eukaryotic CNPase enzyme, the active-site histidine residues are proposed to jointly coordinate the phosphate group for the chemistry to proceed and also participate directly in the reaction (20, 34). The structural studies of CNPase reveal that the mechanism appears to be accompanied by conformational changes that, at least in part, reposition residues that are involved in binding to and properly positioning the substrate (20, 34). Ultimately, insights into potential substrates, further understanding of Sts PDE domain–substrate interactions, and a proposed Sts PDE reaction mechanism, await additional molecular and structural analysis.

Full-length Sts-1, including the entire Sts PDE domain and the two catalytic histidine residues within the 2H phosphoesterase motif, has been highly conserved throughout metazoan evolution. Interestingly, whereas the *Sts* gene is present in some of the most primitive multicellular organisms (*e.g.* the demosponge *Amphimedon queenslandica*), it is absent in the genomes of unicellular choanoflagellates and other more primitive eukaryotes. Therefore, from an evolutionary perspective, one can speculate that sometime during the transition to multicellularity, a unique Sts PDE-like enzyme evolved from an ancestral 2H-phosphesterase enzyme and was eventually incorporated into full-length Sts as one of four functional domains. The high degree of Sts PDE-domain conservation between distant evolutionary orthologues strongly supports the hypothesis that Sts_{PDE} function is vital to the overall role of Sts as a regulator of intracellular signal transduction pathways.

Although full mechanistic insights await further analysis, our current data indicate that Sts-1_{PDE} negatively regulates pathways downstream of select surface receptors. Interestingly, the C-terminal HP domain of Sts-1 also has a role in negatively regulating the activation of different receptor-initiated pathways by targeting key receptor proximal kinases for dephosphorylation. In the case of TCR signaling, the Sts-1 phosphatase domain targets Zap-70 tyrosine kinase activity, whereas in the case of other diverse receptors, Sts-1 targets the Zap-70 homologue Syk. It will be important to determine whether Sts_{PDE} and Sts_{HP} function independently or together in a cooperative manner within the same biochemical pathway. Additional clarity will be provided by identifying the *bona fide* intracellular substrate(s) of Sts-1_{PDE}. Although we utilized 2′,3′-cyclic NADP for our analysis to demonstrate Sts-1 PDE catalytic activity, NADcP is not considered an endogenous cellular compound. With regard to the natural substrate(s) of Sts-1_{PDE}, it is interesting to speculate that an unidentified cyclic nucleotide within cells could be processed by Sts-1_{PDE} to yield a regulatory factor that participates in the regulation of intracellular signaling. Studies are currently in progress to identify substrates, relevant cellular signaling pathways, and effector responses that are regulated by Sts-1_{PDE}. These studies will help determine how the Sts PDE domain contributes to the regulation of important cellular responses such as the expression of key cytokine molecules by activated T cells. Finally, considering the role that Sts plays in host immune modulation, it is also important to acknowledge the unique properties of the Sts PDE domain as a possible target for the development of small molecule therapeutics.

Experimental procedures

Mouse strains, cell lines, and cDNAs

The generation of mice containing the Sts mutations, backcrossed 10 generations onto the C57/B6 background, has been described (38). The mice were housed and bred in the Stony Brook University Animal Facility under specific pathogen-free conditions. All mice were maintained in accordance with Stony Brook University Division of Laboratory Animal Resources guidelines, and all animal experiments were approved by the Stony Brook University Institutional Animal Care and Use Committee.

HEK293 cells were cultured in Dulbecco's modified Eagle's medium (Invitrogen) supplemented with 10% fetal bovine

serum, 100 units/ml penicillin, and 100 μg/ml streptomycin. Jurkat cells were maintained in RPMI 1640 medium (Invitrogen) supplemented with 10% fetal bovine serum, 2 mM glutamine, 100 units/ml penicillin, and 100 μg/ml streptomycin. All cDNA mutants were constructed by PCR mutagenesis and sequenced to confirm the presence of the desired mutation and the absence of additional mutations.

All chemicals were obtained from Sigma–Aldrich, were of the highest purity available, and were used without further purification. Nucleotides were obtained from the following sources: 2′,3′-NADcP, 2′,3′-cAMP, pApA, c-(ApGp), c [A (2′,5′) pG (2′,5′) p], c [A (2′,5′) pA (2′,5′) p], c [G (2′,5′) pA (3′, 5′) p], and 2′,3′-cGAMP from BIOLOG Life Science Institute; cyclic adenosine diphosphate ribose and 3′-NADP from Sigma–Aldrich; 2′,3′-cCMP from Santa Cruz Biotechnology; 3′,5′-cGMP, from Chem-Impex International Inc.; and 2′-NADP from Alfa Aesar.

Luciferase assays

Jurkat cells were transfected via electroporation (Bio-Rad) with Sts-1 expression plasmids, a firefly luciferase expression construct driven by NFAT-binding sequences and a *Renilla* luciferase construct for normalization. 24 h post-transfection, the cells were stimulated by plating on OKT3-coated 96-well plates at a density of 0.2×10^6 cells/well for 6 h, after which luciferase activities were determined using the Dual-Luciferase reporter assay system (Promega). HEK293 cells were plated at a density of 0.3×10^6 cells/well of a 24-well plate and allowed to adhere overnight. The cells were then transfected with Dectin-1, Syk, and Sts-1 expression plasmids and firefly and *Renilla* luciferase constructs. At 24 h post-transfection, the cells were stimulated by the addition of 200 μg zymosan/well for 6 h. Luciferase activities were determined as described above, in triplicate (Jurkat cells) or duplicate (HEK293 cells).

Cloning, expression, and protein purification of the PDE fragment and full-length sts-1

The Sts-1 PDE fragment (Sts-1_{PDE}) was expressed and purified based on an established protocol (41). In brief, the cDNA fragment encoding Sts-1_{PDE} (residues 84−256) was amplified and cloned as a His-tagged protein in the pDB.His.TRX fusion vector (DNASU), which expresses the protein with an N-terminal thioredoxin fusion. The protein was expressed in *E. coli* strain BL21(DE3) at 18 °C after induction at 0.1 mM isopropyl β-D-thiogalactopyranoside. The cell pellet was resuspended in the lysis buffer (20 mM TES, pH 6.8, 500 mM NaCl, 10% glycerol, and 10 mM imidazole) and purified by nickel– nitrilotriacetic acid column (Qiagen). The hexahistine tag and TRX fusion protein were removed from the eluted protein by tobacco etch virus protease, and the resultant protein mixture was run over Ni–nitrilotriacetic acid–agarose once again to remove the hexahistidine-tagged TRX and tobacco etch virus protease. The protein was further purified by size-exclusion chromatography using a SRT-10 SEC-300 (Sepax) column in 20 mM Tris buffer (pH 8.0) and 200 mM NaCl. All mutants were generated by PCR-based site-directed mutagenesis. The mutant proteins hSts-1_{PDE} H126A and hSts-1_{PDE} H212A were purified using the same protocol as the WT hSts-1PDE. Similarly, the full-length human Sts-1 (Sts-1_F) was cloned into the pDB.His.TRX vector, expressed using the same method, and purified the same way as hSts-1PDE.

Western blotting analysis

Transfected/infected cells were lysed in ice-cold lysis buffer (50 mM Tris-HCl, pH 7.6, 150 mM NaCl, 5 mM EDTA, 1 mM EGTA, 1% Triton X-100, 0.2 mM pervanadate, 0.5 mg/ml phenylmethylsulfonyl fluoride, and 1× Roche protease inhibitor mixture) and clarified by centrifugation for 15 min at 13,200 rpm. Lysates were resolved on 7.5% SDS-PAGE gels and electrotransferred onto nitrocellulose membranes (Whatman). After blocking with 3% BSA in Tris-buffered saline, the blots were probed with anti-FLAG (M2 mAb; Sigma) or anti-Syk (clone SYK-01 mAb; BioLegend, Inc.) antibodies followed by appropriate IR dye–conjugated secondary antibodies. Signals were detected using the Odyssey IR imaging system (LI-COR).

In vitro phosphatase assay

For recombinant proteins, phosphatase activity analysis was performed using the established protocol (41). Briefly, 1 mM of pNPP was used as a substrate to quantify the phosphatase activities of Sts-1_{PDE} and Sts-1_F. The appearance of the product, *p*-nitrophenol, was monitored at 405 nm over time to determine the kinetics of the reaction. For full-length Sts-1 expressed in HEK293 cells, the cells were lysed in ice-cold buffer, and Sts-1 proteins were immunoprecipitated following addition of anti-FLAG antibody for 2 h at 4 °C, followed by 1 h at 4 °C with protein A–Sepharose beads (Sigma). The beads were washed three times in assay buffer (25 mM Hepes, pH 7.2, 50 mM NaCl, 0.5 mM β-mercaptoethanol 2.5 mM EDTA, and 0.1 mg/ml BSA) and incubated in a 200-μl reaction mixture containing assay buffer with 1 mM of pNPP for 15 min at 37 °C. The solution was sampled every 5 min, and reaction aliquots were placed into a 96-well plate containing 10 μl of 1 M NaOH to stop the reaction. Phosphate hydrolysis of pNPP was determined by measuring absorbance at 405 nm on a Filtermax F3 plate reader (Molecular Devices). The results displayed are averages of three experiments.

HPLC-based phosphodiesterase assay

The 2′,3′-PDE activities of Sts-1 were determined with 2′,3′-NADcP as a substrate followed by separation by HPLC to identify and quantify the products. In brief, the 2′,3′-NADcP stock (100 mM in water) was diluted with 80 μl of reaction buffer (100 mM Bis-Tris, pH 7.2, 200 mM NaCl). Purified proteins (Sts-1_{PDE}, Sts-1_F, or mutants) and water was added into the reaction mixture to a total volume of 100 μl. The reaction mixture was incubated at 22 °C for the indicated time and then terminated by boiling the samples for 2 min, followed by centrifugation in 0.5-ml centrifugal filters with a molecular mass cutoff of 10 kDa (Amicon) to remove proteins. The filtrate was diluted with water and loaded onto a Zorbax Eclipse Plus C18 4.6 × 100-mm analytical HPLC column running on an Agilent 1100 HPLC. The 2′,3′-NADcP and its hydrolyzed products 2′-NADP and 3′-NADP were eluted with a linear gradient of 0–

100% methanol in the running buffer (10 mM tetrabutylammonium hydroxide, 10 mM KH_2PO_4, pH 6.1) over a period of 20 min at a flow rate of 1 ml/min. Authentic standards of 2′-NADP and 3′-NADP were used to identify the retention times of these compounds and spiking experiments, in which 1 nmol of the compound was added to the complete reaction, and were used to confirm that the presumed product co-eluted with the authentic standard.

To determine the kinetic parameters for the PDE activity of Sts-1_{PDE}, 9 μM Sts-1_{PDE} was added to varying concentrations of 2′,3′-NADcP (1 – 40 mM), and aliquots were removed and measured as described above at two time points to ensure linearity of the reaction progress. The production of 3′-NADP was quantified by integrating the product peak in the chromatogram. The rate of production of 3′-NADP was calculated from the ratio of 3′-NADP to total 2′,3′-NADcP + 2′-NADP + 3′-NADP. The rates of Reeves, production at each concentration were plotted and fit with the Michaelis–Menten equation to determine the kinetic constants. To assess temperature dependence, the reaction was carried out as described, while incubating over a range of temperatures from 20 to 40 °C. To determine whether the enzyme activity showed dependence on divalent cations, we preincubated the enzyme for 30 min with 2 mM of either $MnCl_2$, $ZnCl_2$, $NiCl_2$, $CoCl_2$, or $MgCl_2$ before initiating the reaction.

T-cell culture, retroviral infection, and intracellular cytokine analysis

To obtain primary T cells, dissected spleens from *Sts*$^{-/-}$ mice were crushed in PBS containing 2% FCS, red blood cells were lysed by the addition of ACK lysis buffer (pH 7.2), and debris was removed by straining through a 70-μm filter (Becton Dickinson). Splenocytes were cultured for 24 h in the presence of 1 μg/ml anti-CD3 (145-2C11) and 1 units/ml IL-2 (Peprotech) and then spin-infected with a retrovirus carrying a bicistronic cassette expressing the gene of interest (WT or mutant *Sts-1*) and GFP downstream of an IRES. Infected T cells were allowed to grow 48 h in the presence of IL2, and 1×10^6 cells were then plated and stimulated with the indicated amount of anti-CD3 antibody. Following 4 h of stimulation in the presence of 0.1 μg/ml brefeldin A, the cells were processed for intracellular IFNγ staining using a Cytofix/Cytoperm fixation/permeabilization kit (BD Biosciences) according to the manufacturer's instructions. GFP$^+$ cells were analyzed for IFNγ expression using a BD FACSCalibur flow cytometer (38).

Data availability

All data presented in this article are contained within the article.

Acknowledgments—We thank Laurie Levine and the Stony Brook Department of Laboratory Animal Services for help with animal care.

Author contributions—Y. Y., D. F., W. Z., N. K., and J. B. F. investigation; J. B. F. and N. C. formal analysis; J. B. F. and N. C. supervision; J. B. F. and N. C. funding acquisition; J. B. F. and N. C. methodology; J. B. F. and N. C. writing-original draft; J. B. F. and N. C. writing-review and editing; N. C. conceptualization; N. C. project administration.

Funding and additional information—This work was supported by NIAID, National Institutes of Health Grants R01AI141592 (to N. C. and J. B. F.), R21AI120859 (to N. C. and J. B. F.), and R21AI133381 (to N. C.), as well as by the NHLBI, National Institutes of Health Grant U01HL127522. In addition, parts of this work were supported by NIGMS, National Institutes of Health Grant R35GM124898 (to J. B. F.). Additional support was provided by Stony Brook University, the Stony Brook University Center for Biotechnology (a New York State Center for Advanced Technology), Cold Spring Harbor Laboratory, Brookhaven National Laboratory, the Feinstein Institute for Medical Research, and the Hormel Foundation. The content is solely the responsibility of the authors and does not necessarily represent the official views of the National Institutes of Health.

Conflict of interest—The authors declare that they have no conflicts of interest with the contents of this article.

Abbreviations—The abbreviations used are: TCR, T-cell receptor; pNPP, p-nitrophenyl phosphate; HP, histidine phosphatase; 2H, 2-histidine; PDE, phosphodiesterase; NADcP, 2′,3′-cyclic NADP; UBA, ubiquitin association; SH, Src homology; CNPase, 2′,3′-cyclic nucleotide 3′-phosphodiesterase; IFN, interferon; TES, 2-{[2-hydroxy-1,1-bis(hydroxymethyl)ethyl]amino}ethanesulfonic acid.

References

1. Cantrell, D. (2015) Signaling in lymphocyte activation. *Cold Spring Harb. Perspect. Biol.* **7,** a018788 CrossRef
2. Ogawa, S., and Abe, R. (2019) Signal transduction via co-stimulatory and co-inhibitory receptors. *Adv. Exp. Med. Biol.* **1189,** 85–133 CrossRef Medline
3. Kozicky, L. K., and Sly, L. M. (2015) Phosphatase regulation of macrophage activation. *Semin. Immunol.* **27,** 276–285 CrossRef Medline
4. Futosi, K., and Mócsai, A. (2016) Tyrosine kinase signaling pathways in neutrophils. *Immunol. Rev.* **273,** 121–139 CrossRef Medline
5. Tsygankov, A. Y. (2020) TULA proteins as signaling regulators. *Cell Signal.* **65,** 109424 CrossRef Medline
6. Carpino, N., Turner, S., Mekala, D., Takahashi, Y., Zang, H., Geiger, T. L., Doherty, P., and Ihle, J. N. (2004) Regulation of ZAP-70 activation and TCR signaling by two related proteins, Sts-1 and Sts-2. *Immunity* **20,** 37–46 CrossRef Medline
7. Yang, M., Chen, T., Li, X., Yu, Z., Tang, S., Wang, C., Gu, Y., Liu, Y., Xu, S., Li, W., Zhang, X., Wang, J., and Cao, X. (2015) K33-linked polyubiquitination of Zap70 by Nrdp1 controls CD8$^+$ T cell activation. *Nat. Immunol.* **16,** 1253–1262 CrossRef Medline
8. Hu, H., Wang, H., Xiao, Y., Jin, J., Chang, J. H., Zou, Q., Xie, X., Cheng, X., and Sun, S. C. (2016) Otud7b facilitates T cell activation and inflammatory responses by regulating Zap70 ubiquitination. *J. Exp. Med.* **213,** 399–414 CrossRef Medline
9. Thomas, D. H., Getz, T. M., Newman, T. N., Dangelmaier, C. A., Carpino, N., Kunapuli, S. P., Tsygankov, A. Y., and Daniel, J. L. (2010) A novel histidine tyrosine phosphatase, TULA-2, associates with Syk and negatively regulates GPVI signaling in platelets. *Blood* **116,** 2570–2578 CrossRef Medline
10. de Castro, R. O., Zhang, J., Groves, J. R., Barbu, E. A., and Siraganian, R. P. (2012) Once phosphorylated, tyrosines in carboxyl terminus of protein-tyrosine kinase Syk interact with signaling proteins, including TULA-2, a negative regulator of mast cell degranulation. *J. Biol. Chem.* **287,** 8194–8204 CrossRef Medline
11. Frank, D., Naseem, S., Russo, G. L., Li, C., Parashar, K., Konopka, J. B., and Carpino, N. (2018) Phagocytes from mice lacking the Sts phosphatases

have an enhanced antifungal response to *Candida albicans*. *mBio* **9,** e00782-18 CrossRef Medline
12. Inshaw, J. R. J., Cutler, A. J., Burren, O. S., Stefana, M. I., and Todd, J. A. (2018) Approaches and advances in the genetic causes of autoimmune disease and their implications. *Nat. Immunol.* **19,** 674–684 CrossRef Medline
13. Diaz-Gallo, L. M., Sánchez, E., Ortego-Centeno, N., Sabio, J. M., García-Hernández, F. J., de Ramón, E., Gonzalez-Gay, M. A., Torsten, W., Anders, H. J., Gonzalez-Escribano, M. F., and Martin, J. (2013) Evidence of new risk genetic factor to systemic lupus erythematosus: the *UBASH3A* gene. *PLoS One* **8,** e60646 CrossRef Medline
14. Todd, J. A. (2018) Evidence that UBASH3 is a causal gene for type 1 diabetes. *Eur. J. Hum. Genet.* **26,** 925–927 CrossRef Medline
15. Naseem, S., Frank, D., Konopka, J. B., and Carpino, N. (2015) Protection from systemic *Candida albicans* infection by inactivation of the Sts phosphatases. *Infect. Immun.* **83,** 637–645 CrossRef Medline
16. Parashar, K., Kopping, E., Frank, D., Sampath, V., Thanassi, D. G., and Carpino, N. (2017) Increased resistance to intradermal *Francisella tularensis* LVS infection by inactivation of the Sts phosphatases. *Infect. Immun.* **85,** e00406-17 CrossRef Medline
17. Chen, M. J., Dixon, J. E., and Manning, G. (2017) Genomics and evolution of protein phosphatases. *Sci. Signal.* **10,** eaag1796 CrossRef Medline
18. Rigden, D. J. (2008) The histidine phosphatase superfamily: structure and function. *Biochem. J.* **409,** 333–348 CrossRef Medline
19. Mazumder, R., Iyer, L. M., Vasudevan, S., and Aravind, L. (2002) Detection of novel members, structure–function analysis and evolutionary classification of the 2H phosphoesterase superfamily. *Nucleic Acids Res.* **30,** 5229–5243 CrossRef Medline
20. Myllykoski, M., Raasakka, A., Han, H., and Kursula, P. (2012) Myelin 2′,3′-cyclic nucleotide 3′-phosphodiesterase: active-site ligand binding and molecular conformation. *PLoS One* **7,** e32336 CrossRef Medline
21. Hofmann, A., Zdanov, A., Genschik, P., Ruvinov, S., Filipowicz, W., and Wlodawer, A. (2000) Structure and mechanism of activity of the cyclic phosphodiesterase of Appr>p, a product of the tRNA splicing reaction. *EMBO J.* **19,** 6207–6217 CrossRef Medline
22. Wang, L. K., and Shuman, S. (2005) Structure–function analysis of yeast tRNA ligase. *RNA* **11,** 966–975 CrossRef Medline
23. Remus, B. S., Jacewicz, A., and Shuman, S. (2014) Structure and mechanism of *E. coli* RNA 2′,3′-cyclic phosphodiesterase. *RNA* **20,** 1697–1705 CrossRef Medline
24. Myllykoski, M., Seidel, L., Muruganandam, G., Raasakka, A., Torda, A. E., and Kursula, P. (2016) Structural and functional evolution of 2′,3′-cyclic nucleotide 3′-phosphodiesterase. *Brain Res.* **1641,** 64–78 CrossRef Medline
25. Lee, J., Gravel, M., Gao, E., O'Neill, R. C., and Braun, P. E. (2001) Identification of essential residues in 2′,3′-cyclic nucleotide 3′-phosphodiesterase: chemical modification and site-directed mutagenesis to investigate the role of cysteine and histidine residues in enzymatic activity. *J. Biol. Chem.* **276,** 14804–14813 CrossRef Medline
26. Kanai, A., Sato, A., Fukuda, Y., Okada, K., Matsuda, T., Sakamoto, T., Muto, Y., Yokoyama, S., Kawai, G., and Tomita, M. (2009) Characterization of a heat-stable enzyme possessing GTP-dependent RNA ligase activity from a hyperthermophilic archaeon, *Pyrococcus furiosus*. *RNA* **15,** 420–431 CrossRef Medline
27. Macian, F. (2005) NFAT proteins: key regulators of T-cell development and function. *Nat. Rev. Immunol.* **5,** 472–484 CrossRef Medline
28. Mikhailik, A., Ford, B., Keller, J., Chen, Y., Nassar, N., and Carpino, N. (2007) A phosphatase activity of Sts-1 contributes to the suppression of TCR signaling. *Mol. Cell* **27,** 486–497 CrossRef Medline
29. San Luis, B., Nassar, N., and Carpino, N. (2013) New insights into the catalytic mechanism of histidine phosphatases revealed by a functionally essential arginine residue within the active site of the Sts phosphatases. *Biochem. J.* **453,** 27–35 CrossRef Medline
30. Drummond, R. A., and Brown, G. D. (2013) Signalling C-type lectins in antimicrobial immunity. *PLoS Pathog.* **9,** e1003417 CrossRef Medline
31. Sancho, D., and Reis e Sousa, C. (2012) Signaling by myeloid C-type lectin receptors in immunity and homeostasis. *Annu. Rev. Immunol.* **30,** 491–529 CrossRef Medline
32. Kerrigan, A. M., and Brown, G. D. (2011) Syk-coupled C-type lectins in immunity. *Trends Immunol* **32,** 151–156 CrossRef Medline
33. Del Fresno, C., Iborra, S., Saz-Leal, P., Martínez-López, M., and Sancho, D. (2018) Flexible signaling of myeloid C-type lectin receptors in immunity and inflammation. *Front. Immunol.* **9,** 804 CrossRef Medline
34. Raasakka, A., Myllykoski, M., Laulumaa, S., Lehtimaki, M., Hartlein, M., Moulin, M., Kursula, I., and Kursula, P. (2015) Determinants of ligand binding and catalytic activity in the myelin enzyme 2′,3′-cyclic nucleotide 3′-phosphodiesterase. *Sci. Rep.* **5,** 16520 CrossRef Medline
35. Sogin, D. C. (1976) Cyclic NADP as a substrate for 2′,3′-cyclic nucleotide 3′-phosphohydrolase. *J. Neurochem.* **27,** 1333–1337 CrossRef Medline
36. Kato, K., Omura, H., Ishitani, R., and Nureki, O. (2017) Cyclic GMP-AMP as an endogenous second messenger in innate immune signaling by cytosolic DNA. *Annu. Rev. Biochem.* **86,** 541–566 CrossRef Medline
37. Motwani, M., Pesiridis, S., and Fitzgerald, K. A. (2019) DNA sensing by the cGAS-STING pathway in health and disease. *Nat. Rev. Genet.* **20,** 657–674 CrossRef Medline
38. San Luis, B., Sondgeroth, B., Nassar, N., and Carpino, N. (2011) Sts-2 is a phosphatase that negatively regulates zeta-associated protein (ZAP)-70 and T cell receptor signaling pathways. *J. Biol. Chem.* **286,** 15943–15954 CrossRef Medline
39. Mitsutomi, S., Akimitsu, N., Sekimizu, K., and Kaito, C. (2019) Identification of 2H phosphoesterase superfamily proteins with 2′-CPDase activity. *Biochimie* **165,** 235–244 CrossRef Medline
40. Tanaka, N., Chakravarty, A. K., Maughan, B., and Shuman, S. (2011) Novel mechanism of RNA repair by RtcB via sequential 2′,3′-cyclic phosphodiesterase and 3′-phosphate/5′-hydroxyl ligation reactions. *J. Biol. Chem.* **286,** 43134–43143 CrossRef Medline
41. Zhou, W., Yin, Y., Weinheimer, A. S., Kaur, N., Carpino, N., and French, J. B. (2017) Structural and functional characterization of the histidine phosphatase domains of human Sts-1 and Sts-2. *Biochemistry* **56,** 4637–4645 CrossRef Medline